Accepted Manuscript

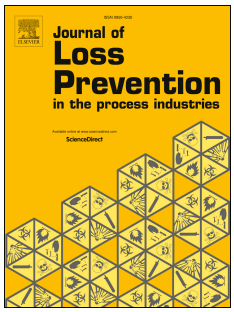

Numerical modelling of deflagration to detonation transition in inhomogeneous hydrogen/air mixtures

Reza Khodadadi Azadboni, Jennifer X. Wen, Ali Heidari, Changjian Wang

PII: S0950-4230(17)30393-5

DOI: 10.1016/j.jlp.2017.04.024

Reference: JLPP 3490

To appear in: *Journal of Loss Prevention in the Process Industries*

Received Date: 5 October 2016

Revised Date: 20 April 2017

Accepted Date: 23 April 2017

Please cite this article as: Azadboni, R.K., Wen, J.X., Heidari, A., Wang, C., Numerical modelling of deflagration to detonation transition in inhomogeneous hydrogen/air mixtures, *Journal of Loss Prevention in the Process Industries* (2017), doi: 10.1016/j.jlp.2017.04.024.

Numerical Modelling of Deflagration to Detonation Transition in Inhomogeneous Hydrogen/Air Mixtures

Reza Khodadadi Azadboni [a], Jennifer X. Wen [b, *], Ali Heidari [a] & Changjian Wang [c]

*corresponding author: E-mail: *Jennifer.Wen@warwick.ac.uk*

[a] Fire, Explosion and Fluid Dynamics Research Team, School of Mechanical & Automotive Engineering, Kingston University London, SW15 3DW, UK

[b] Warwick FIRE, School of Engineering, University of Warwick, Coventry, CV4 7AL, UK

[c] School of Civil Engineering, Hefei University of Technology, Hefei, 230009, Anhui, China

Abstract

Explosions in homogeneous reactive mixtures have been widely studied both experimentally and numerically. However, in practice, combustible mixtures are usually inhomogeneous and subject to both vertical and horizontal concentration gradients. There is still very limited understanding of the explosion characteristics in such situations. The present study aims to investigate deflagration to detonation transition (DDT) in such mixtures. Two cases in a horizontal obstructed channel with 30% and 60% blockage ratios filled with hydrogen/air mixture with vertical concentration gradients are numerically studied. These cases were experimentally investigated by Boeck et al. (2015), and hence some measurements are available for model validation. A density-based solver within the OpenFOAM CFD toolbox is developed and used. To evaluate the convective fluxes contribution, the Harten–Lax–van Leer–Contact (HLLC) scheme is used for shock capturing. The compressible Navier–Stokes equations with a single step Arrhenius reaction are solved. The numerical results are in good qualitative and quantitative agreement with the experiments. The predictions show that the overpressure at the DDT transition stage is higher in the non-uniform mixtures than that in homogeneous mixtures under similar conditions. It is also found that increasing the blockage ratio from 30% to 60% resulted in faster flame propagation and lower propensity to DDT. The Baroclinic torque and the resulting Richtmyer–Meshkov (RM) instability are also analyzed in relation to flame acceleration and DDT.

Keywords: *Hydrogen safety, Explosion, DDT, Inhomogeneous mixture, Instability*

1. Introduction and background

Flame acceleration (FA) and deflagration to detonation transition (DDT) in channels have been extensively studied. Most of these studies were conducted for industrial safety and intending to understanding the mechanisms of flame propagation. Much effort has been dedicated to understanding the phenomena related to FA and DDT (Ersen, 2004). Thomas (2012) has given a comprehensive study on various forms of DDT phenomena, and differentiated the terminology between the macroscopic and the microscopic DDT. He considered the large scale macroscopic DDT to include the process from accelerating deflagration up to a propagating detonation; and the small-scale microscopic DDT initiate the actual onset of detonation at the point where the combustion process changes from diffusion controlled to shock heating controlled. Looking from this standpoint, the present work concerns the large-scale macroscopic DDT.

Industrial pipelines, equipment transport and storage, involve a wide range of hazardous materials which are combustible. Their existence poses a risk, particularly when an ignition source is available or when the temperature or pressure go over the self-ignition limitations (Ersen, 2004). There is still very little understanding about the effect of mixture inhomogeneity on explosion behavior and the potential for DDT.

Boeck et al. (2015) recently studied flame acceleration and DDT in a channel with vertically variable hydrogen concentrations. They illustrated that the flame accelerated faster when it burned in these gradients. The DDT phenomena were also observed as reflected shock waves interacted with the deflagration flame front.

Some theoretical and numerical studies have also been directed towards understanding the evolution and growth of Richtmyer–Meshkov (RM) instability in reactive flows (e.g. Li & Zhang, 1997). The fundamental physics of generation and propagation of RM instability was studied in detail numerically by Brouillette (2012). They examined a shock wave interacting with the interface of two fluids of different densities. Any perturbation on the interface of the flow was found to increase the refraction of the shock wave in the flow field. Generally, the evolution of the initial perturbation along the interface of the flow changes linearly with time (Cloutman and Wehner, 1992). However, while the amplitude increases, it causes heavy fluid accelerating towards the light fluid and bubbles of light fluid "rise" into the heavy fluid (Brouillette, 2012). Moreover, at some points, this can result in "mushrooming" of the spike and the appearance of smaller-scale vortices (Mahmoudi et al., 2013). As a result, a turbulent mixing zone grows among the two fluids (Brouillette, 2012). The mechanism for the increase of perturbations on the interface of the fluid is known as baroclinic vorticity generation, which is due to the misalignment of the density and pressure gradient across the interface ($(\nabla\rho \times \nabla p) / \rho^2$). Its existence leads to surface fluctuations from RM instability at the interface between the burnt and unburnt gases.

This unstable vortex sheet leads to increase in the amplification of the initial perturbations, which can be characterized either by a sinusoidal function of a given wavelength and amplitude (i.e., single mode of RM instability) or a superposition of these perturbations (i.e., multiple mode of RM instability) (Vetter and Sturtevant, 1995). Additionally, probable secondary shocks impacting on the evolving mixing layer can substantially increase the mixing processes (Ukai et al., 2011) and accelerate the transition of the layer to a fully turbulent mixing zone.

Li and Zhang (1997) conducted a detailed numerical investigation of RM instability in two-dimensional (2D) and 3D coordinates and found that, for the same initial amplitude and wavelength, the growth rate of the instability in 2D and 3D models are basically the same and have the same perturbation in the linear regime. However, for the nonlinear regime, the growth rates in the 3D cases were found to be about 20% and 25% larger and faster. Khokhlov et al. (1999), conducted similar numerical investigations and found that in 3D simulations the perturbations of the same wavelength and amplitude grow by a factor of two faster than the 2D case, and the maximum energy release rate was larger by a factor of two. Their findings contradict the results of some other investigations which showed that the trend of instability generation and evolution were the same for both 2D and 3D modeling (Regele, 2013).

Ciccarelli and Dorofeev (2008) experimentally showed that in the fast-turbulent flame regime, the shock-flame interaction is the main mechanism affecting the flame speed. Therefore, because of the interaction of reflected shock waves with the flame, the interface between the burned and unburned gases will be distorted via the baroclinic vorticity generation mechanism. This will triggers the RM instability leading to fine-scale flame wrinkling.

Kholkhlov et al. (1999) also concluded similarly that shock-flame interaction is important to accelerate flames to critical conditions for the onset of detonation. They mentioned that large scale RM instability is the primary mechanism increasing the heat release rate during the interaction of a flame with a single shock through macroscopic flame surface area growth.

Mahmoudi et al. (2013) emphasized the role of hydrodynamic instabilities in the propagation mechanism of detonation. Although they detected self-sustained propagation of detonation in a laboratory experiment, in the numerical investigations, it was only observed in the regions where the turbulent mixing was not resolved, and large unreacted pockets of gas were formed. It can, therefore, be postulated that without the unresolved small-scale instabilities, the detonation wave could not be self-sustained and would fail.

Mazaheri et al. (2012), showed that for regular detonation in the hydrogen-air mixture, hydrodynamic instabilities do not play a role in propagation mechanism of the detonation wave, so there is no need to use a high grid resolution in order to capture the phenomena properly. In the present work we investigate the propagation of hydrogen-air detonation in a very long channel, and thus, resolution of 10 cell per half reaction length (HRL) is enough for analysis based on the available computational resources. (HRL is the length behind the shock for the reaction progress variable to reach one half).

In the present study, numerical investigations were conducted on the propagation mechanism of DDT in the non-homogenous mixture in an obstructed channel with different blockage ratios. This was flowed by the analysis of RM instability and its influence on FA and DDT.

2. Numerical Methods

A density-based solver within OpenFOAM CFD toolbox (OpenFOAM Ltd., 2015) is assembled on the basis of rhoCentralFoam for density based Navier-Stokes equation and reactingFoam for combustion. The Harten–Lax–van Leer–Contact (HLLC) scheme with multidimensional slope limiters (“cellMDLimited” (OpenFOAM Wiki, 2010)) is used for shock capturing (Ettner 2014). Two-dimensional compressible Navier–Stokes equations with a single step Arrhenius reaction are solved. The single-step hydrogen reaction scheme developed by Wang et al., (2012) is used. For code verification, predictions were conducted for the Sod’s shock tube problem (Sod, 1978). As shown in Fig. 1, the predicted pressure and temperature distributions are in excellent agreement with the analytical solutions.

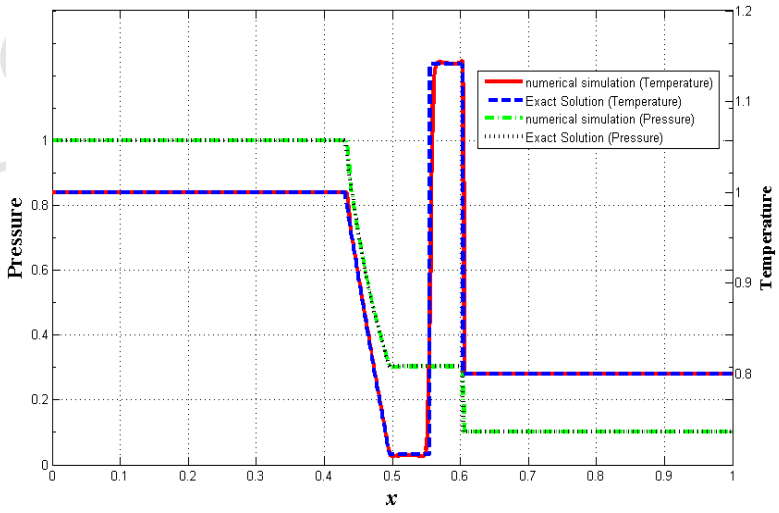

***Fig. 1**. Model verification with the Sod's problem.*

3. The experiments considered

The experiments of Boeck et al. (2015) involving inhomogeneous DDT phenomena of hydrogen-air mixture were chosen for the present study. The experiments were conducted in a horizontal obstructed channel with 30% and 60% blockage ratios. The channel was 60 mm high, 5.4 m long and 300 mm wide, respectively. It was initially filled with the inhomogeneous hydrogen-air mixture, which was on average 30% hydrogen by volume. The initial concentration profile is shown in Figure 3 with concentration gradients in the vertical direction. The ignition was started by a weak spark in the experiment.

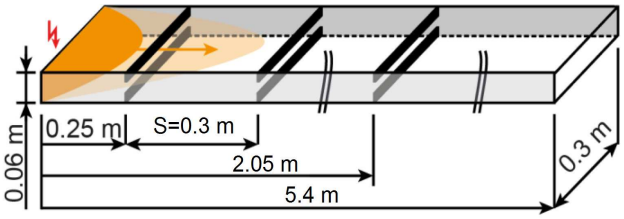

***Fig. 2.** Schematic of the computational domain (Reproduced from Boeck et al., (2015)).*

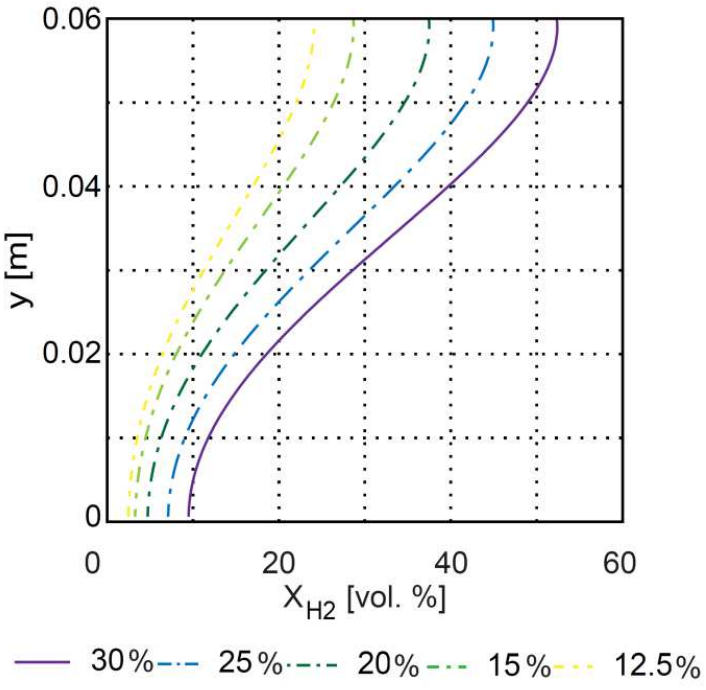

***Fig. 3.** The volumetric hydrogen concentration gradients in the experiments (Reproduced from Boeck et al., (2015)).*

4. Numerical setup

Figure 2 shows the computational domain which represents a smooth closed channel with obstacles. The mixture was initially in ambient pressure and temperature. In order to initiate ignition, a patch of cells within a radius of 10 mm around the point of ignition (x=0, y=0.03m) was set with a temperature of 2400 K and atmospheric pressure.

Several researchers report different values of the half reaction length. This depends on the reaction mechanism and the initial condition of that reaction as well. Gamezo et al. (2007), reported half reaction length of hydrogen-air mixture is 0.01927 cm, however, Kumar et al. (2015), showed that half reaction length of hydrogen-air reaction is different for different reaction mechanism and in their study with changing the initial temperature that varied from 0.02 mm to 0.1 mm. Moreover, as shown by Stamps et al. (1991), the HRL changes considerably with the mixture equivalence ratio. In the present study, the average volumetric hydrogen concentration is 30% which is close to the stoichiometric value with HRL 0.3 mm. However, with the presence of the concentration gradients, the actual equivalence ratio varies from 0.338 to 1.69. According to Fig. 5, the actual HRL would be between 0.3mm (stoichiometric value) and 0.39mm (rich level). Therefore for the majority of the domain, the resolutions should meet the usual practice of between 10 to 14 cells per HRL.

Therefore, the adaptive mesh refinement capability was used with a minimum cell size of 30 µm, giving approximately by average 10 grid points per half reaction length (HRL) in the finest region near the flame and shock fronts.

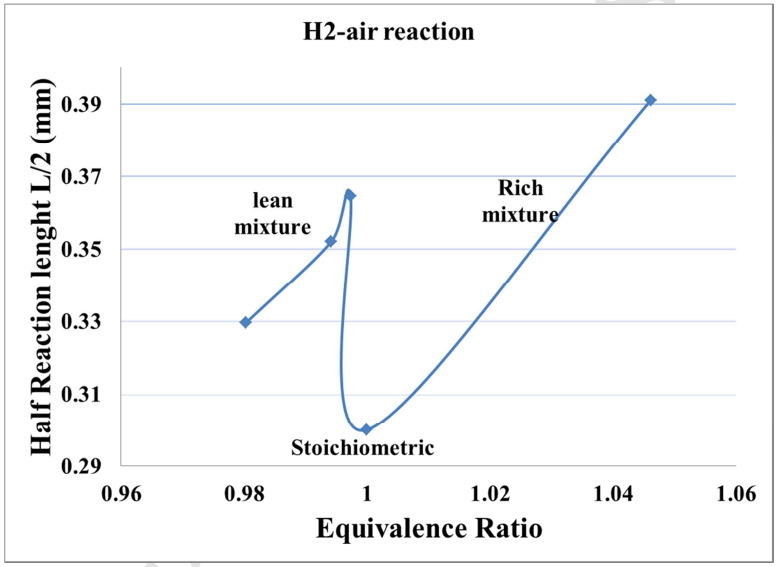

Fig. 4*. The half reaction length of hydrogen-air flame verse equivalence ratio (Reproduced from Stamps et al. (1991)).*

5. Results and discussion

As shown in Figures 5 and 6, the predicted flame position and flame tip speed for both cases are in reasonably good agreement with the measurements of Boeck et al. (2015). It can be seen (Fig. 5) that the flame velocity rises continuously in the obstructed part of the channel (around the 7th obstacle, $x \leq 2.05$ m) due to flame interaction with the obstacles, resulting in combustion-induced expansion and turbulence generation. Then, after the flame passes the 6th obstacle, the flame speed reaches around 2100 m/s, which is around the Chapman-Jouguet (CJ) detonation velocity (1980 m/s) of the stoichiometric hydrogen-air mixture. After the flame and detonation wave pass the last obstacle which is located in x=2.05 m, the flame speed reaches to a maximum of around the 2200 m/s before decreasing slowly.

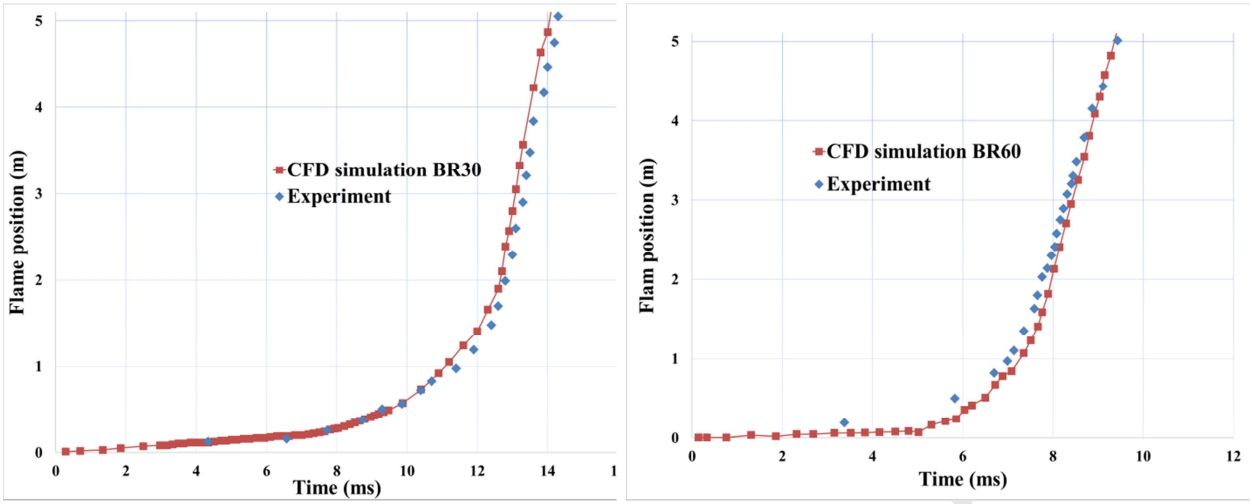

Fig. 5. *Comparison between the predicted and measured flame position for left) BR30% and right) BR60%.*

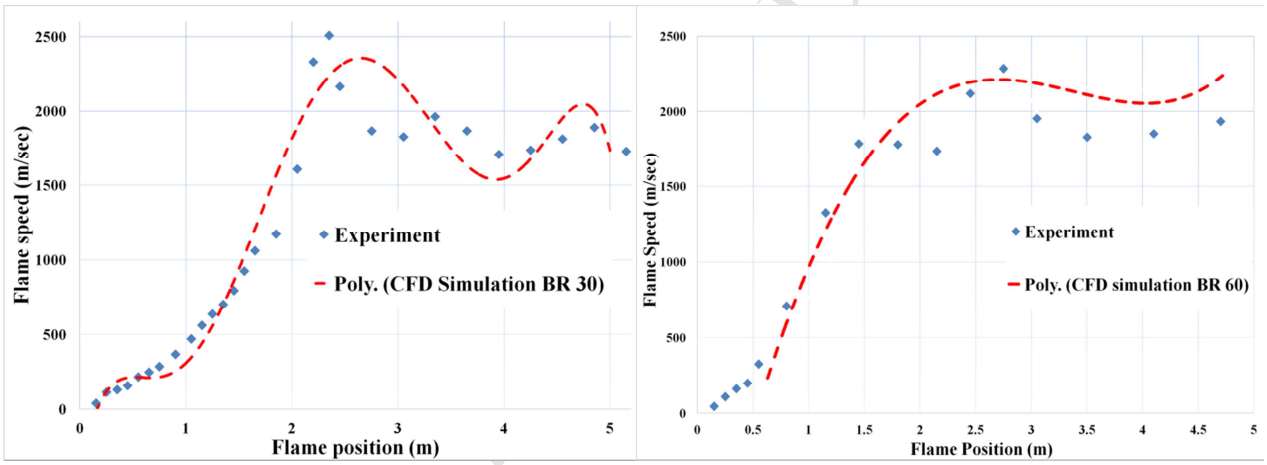

Fig. 6. *Comparison between the predicted and measured flame tip speed for left) BR30% and right) BR60%.*

However, Fig. 5 shows that by increasing the blockage ratio from BR 30 to BR 60, the flame will propagate faster in the channel, but it does not mean the mixture will detonate faster, and for this issue, other parameters should be investigated. From Fig. 6, it can be seen that the maximum flame speed in the case with 30% BR is higher than that in the case with 60% BR (maximum flame speed of BR 30 is 2507 m/s located at x=2.75 and maximum flame speed for BR 60 is 2285 m/s located at x=2.35 m). Also, it can be found that until flame reaches the detonation (around obstacle 6 and 7), always the BR60 case has a higher flame tip velocity than the BR30 case, and after the flame transited to detonation, in average, they have almost the same amount of flame tip speed.

Figure 8 shows the predicted pressure contours in the regions around obstacles 6 and 7, where the first local explosion took place. It can be seen that the first abrupt pressure rise appears next to the obstacle 6 near to the bottom wall at 12.39ms (it also can be seen in Fig. 7).

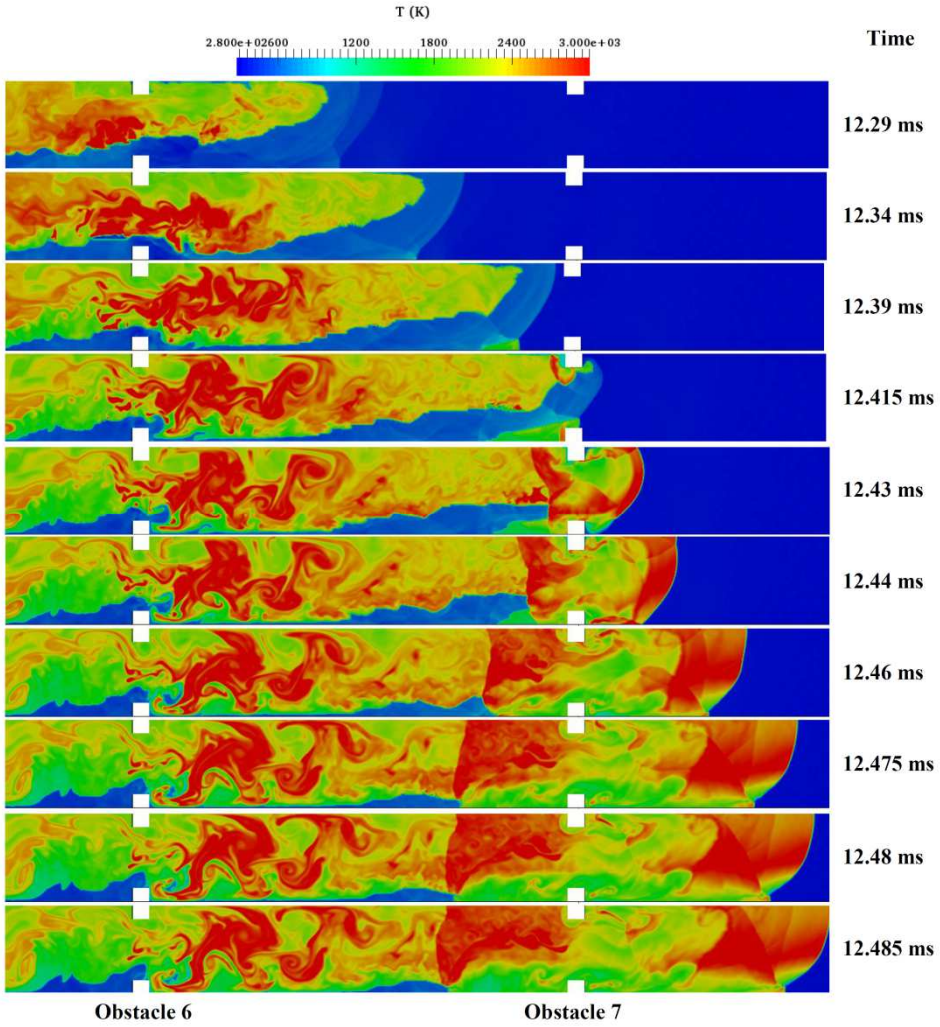

Fig. 7. *Temperature contours of deflagration to detonation for average 30% Vol H2, BR30.*

Figure 7 shows the temperature contour around obstacle 6 and 7 and Fig. 8 shows the pressure contour around these two obstacles. These two pictures illustrate the process of DDT in the 30% BR case. It can be seen that the generated flame propagates faster at the top of the domain where the fuel is richer due to the non-uniformity of the mixture.

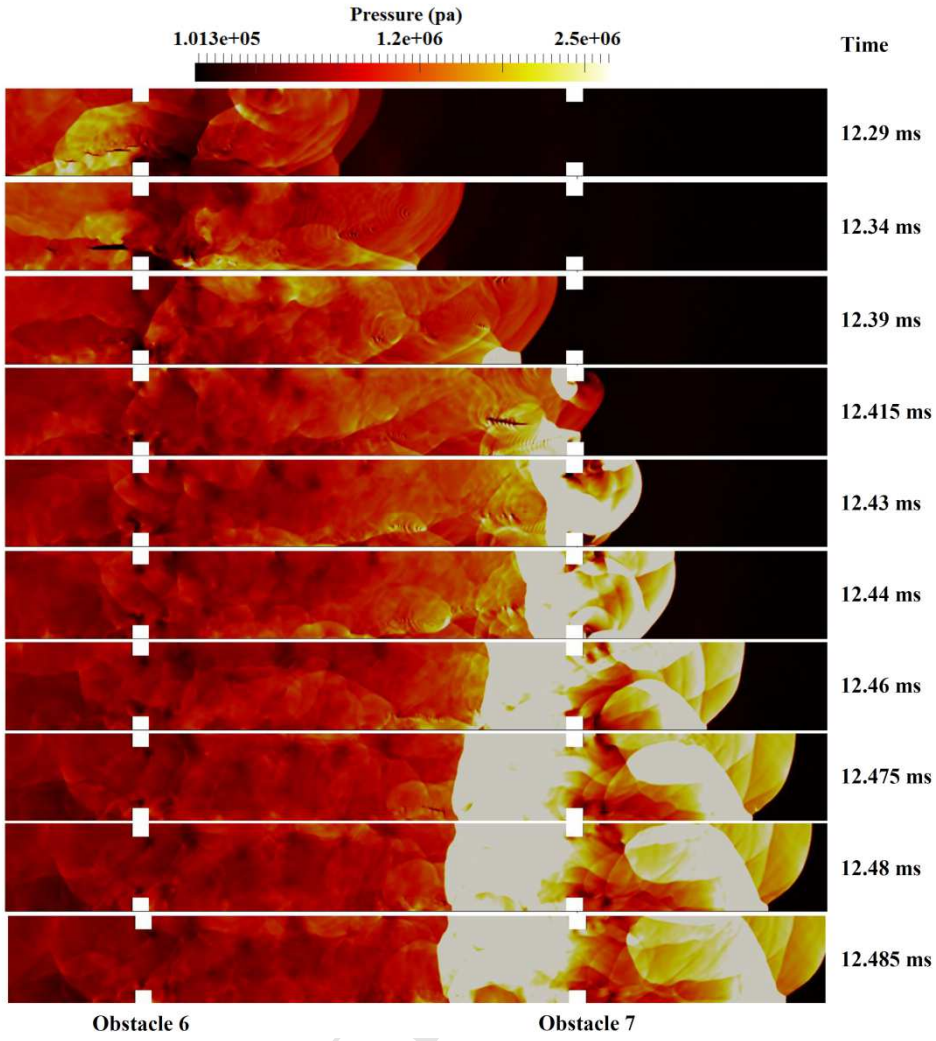

Fig. 8. *Pressure contours of deflagration to detonation for average 30% Vol H2, BR30.*

As shown in Fig. 8, at 12.29 ms, the flame and shock are still detached. From the temperature contour in Fig. 7, it can be seen no localized explosion is formed yet.

The first localized explosion occurred at 12.39ms near the bottom wall where the shock and flame interacted and the mixture was most lean with the volumetric hydrogen concentration being around 10% and the local speed of sound being around 361m/s. The Mach stem can be seen as a normal shock propagating at Mach number Ma = 4.01 near the bottom of the channel, as shown in Fig. 7 and Fig. 8, around the obstacle 7 at 12.39ms. This was followed by a stronger second localized explosion near the top wall as a result of the reflected shock from the top obstacle hitting the flame front (it can be found at 12.415ms). From the next frame, it can be seen that the second local explosion became the main drive for the detonation wave propagation through the rest of the domain. The Mach stem can be seen as a normal shock propagating at Mach number Ma = 4.01 near the bottom of the channel, as shown in Fig. 7 around obstacle 7 at 12.40ms. Moreover, after this time, the leading shock and the flame are coupled indicating that the flame has undergone a transition to detonation.

Fig. 9 shows the temperature contour for the case with 60% BR. Here the first leading shock ahead of the flame front occurred around 8.08 ms but DDT still has not occurred. However, according to Fig. 7 for the 30% BR case, the first shock ahead of the flame front occurred around 12.29 ms, indicating that flame is faster in the 60% BR case. Comparison with the

predictions for the 30% BR case, increasing the blockage ratio in the present configuration has increased the flame speed, but it has also increased the DDT run up distance, therefore reduced the possibility of DDT (as discussed in Fig. 6). Moreover, Fig. 9-b, which illustrates the flame around obstacle 3, shows that RM instability has occurred sooner in this case owing to greater flame speed comparing with the 30% BR case. This is thought to be due to enhanced turbulence mixing caused by interaction with the obstacles.

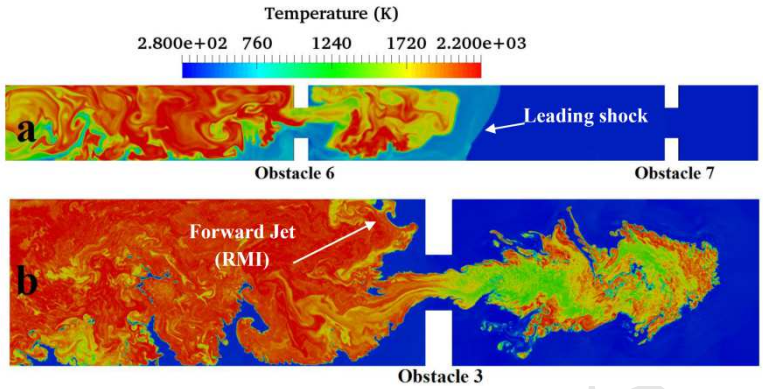

Fig. 9. *The predicted contour of the temperature for BR 60, a) time=8.08ms and b) time=6.49ms.*

Figure 9 shows the evolution of the turbulent deflagration. Some forward and backwards jets can be seen at the interface of the burnt and unburnt gases, illustrating the existence of RM instability. Because of the existence of high gradients of pressure and density, one of the main hydrodynamic instabilities in DDT phenomena, is RM instability. There is a strong misalignment of the density gradient and pressure gradient at the interface between the flame front and pressure wave. This can trigger baroclinic torque ($\nabla\rho \times \nabla p$) which is generated as the results of baroclinic vorticity $\left(\nabla\rho \times \nabla p / \rho^2\right)$ and responsible for RM instability.

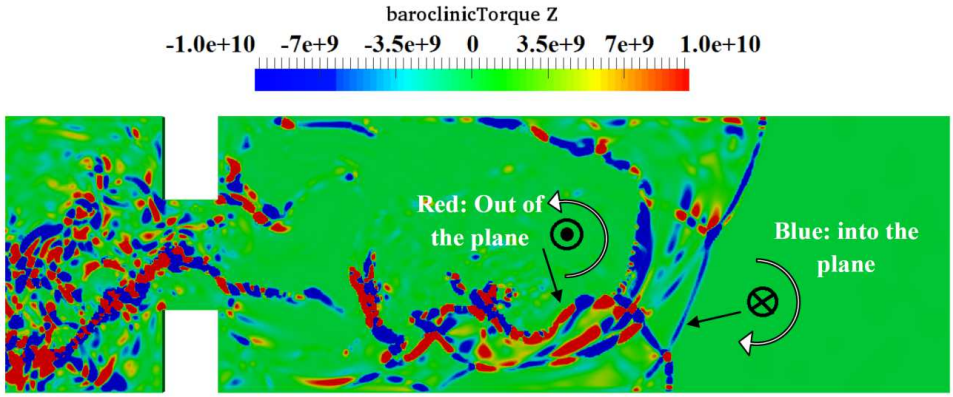

Fig. 10. *The contour of the predicted Baroclinic torque in Z direction for BR 60 and time 8.08 ms.*

This misalignment in a baroclinic torque which generates vorticity can be seen in Fig. 10. As discussed in the introduction, while shock refracts from the interface of burned and unburned gas, a misalignment in the density and pressure gradients occurs. This results in the presentence of baroclinic vorticity through the production of baroclinic torque along the contact discontinuity causing the perturbations to grow in amplitude (Mahmoudi et al., 2013). The misalignments between baroclinic vorticities are caused by the cross-multiplication of gradient of density to the gradient of pressure (the misalignment is illustrated in Fig. 11).

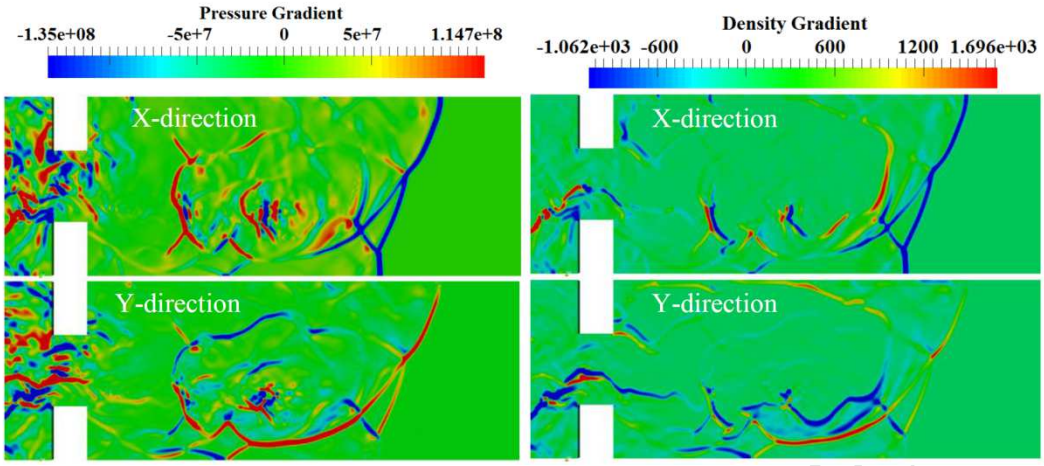

Fig. 11. *Pressure gradient (left), and density gradient (right), in X and Y directions for BR 60 and time 8.08 ms.*

As can be seen from Fig. 11 that in the same direction either X or Y, the pressure and density gradient vectors in the same regions are inline, i.e. they are either both negative or positive. On the other hand, for different directions, these vectors have misalignment. As a result, as shown in Fig. 10, some parts of the baroclinic torque vectors are red (a positive vector which points away from the page), and some parts are blue (a negative vector which points towards the page). These results illustrate the existence of both positive and negative baroclinic vorticities in the flow field.

Figure 12 plots the contours of the predicted baroclinic torque for the region around obstacles 6 and 7 at different times. It is seen that the baroclinic torque increases with time, promoting RM instability, FA and DDT. It can be seen in Fig. 12-(a, b and c), the locations of the maximum values of the baroclinic torque are aligned with those spots where there are Mach stem in the bottom wall. In Fig. 12-d, it can be seen that the DDT occurred at where there is maximum baroclinic torque and RM instability, and also according to Fig. 8, it can be seen that around this time DDT has been occurred.

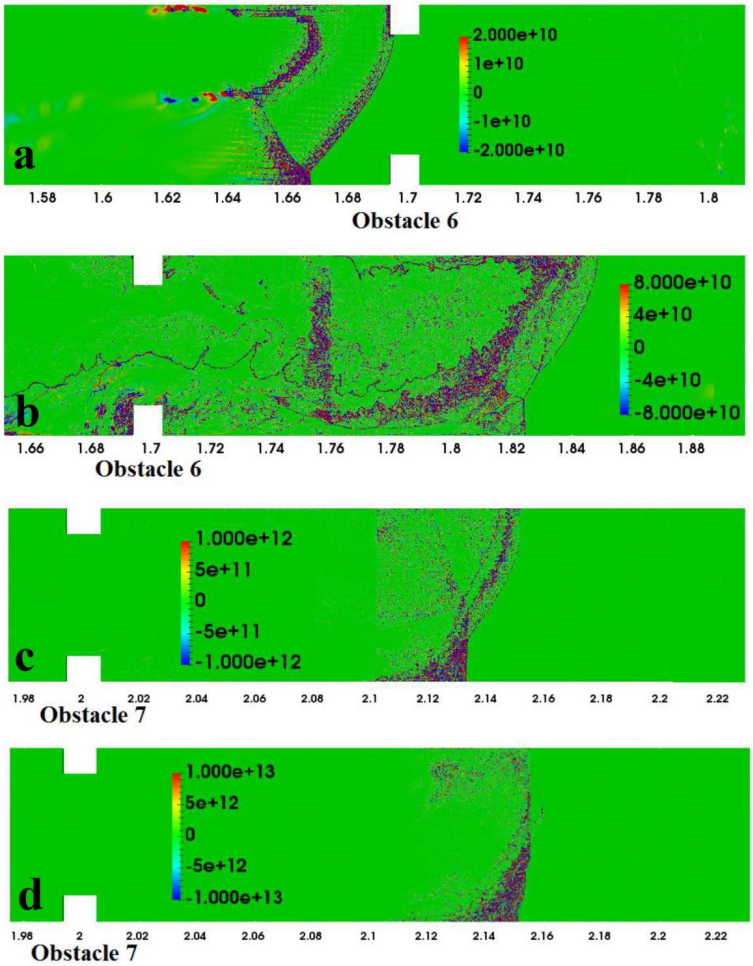

Fig. 12. *The contours of the predicted Baroclinic torque in Z direction for BR 30 and a) time=11.79 ms, b) time=11.91 ms, c) time=12.48 ms and d) time=12.50 ms.*

It can also be seen Fig. 10 and 12 that more baroclinic vorticities are generated in the vicinity of the Mach stem (Mach stem can be seen in Fig. 10 and Fig. 12-b). In other regions, baroclinic torque exists just along the interface between the flame and strong shock waves. The vicinity of the Mach stem and flame shock interfaces are, therefore, the regions most prone to have RM instabilities. This is also evidenced by the presence of forward or backward jets, resulting in mushroom shape flow patterns along the interface.

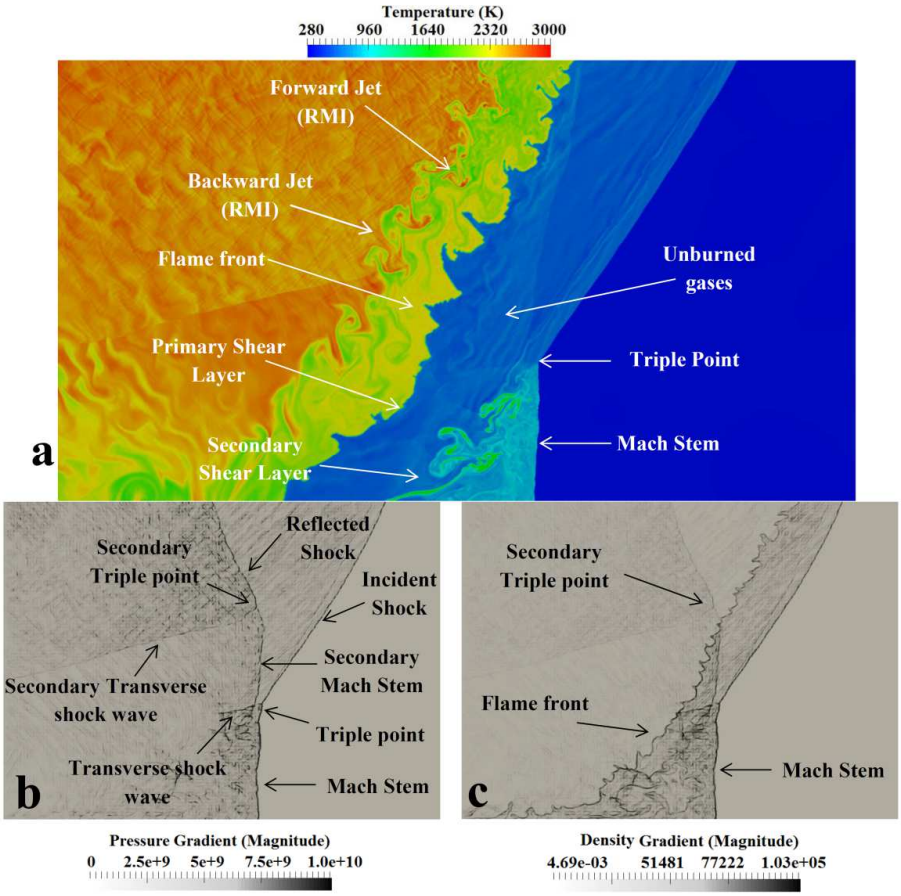

Fig. 13. *RM instability diagram in BR 30 and time=12.49ms, a) The predicted temperature contour illustrating RM instability b) pressure gradient contour and c) density gradient contour.*

Figure 13-a, shows the temperature contour illustrating the occurrence of RM instabilities at the burnt-unburnt gas interface. The typical mushroom shapes RM instability are seen in the form of forward and backward jets. The interaction of the shock with the flame front is also accompanied by the existence of density differences between the burnt and unburnt gases. The backward jets in the primary shear layer propagated into the hot and burned gases and can be consumed shortly in the pool of hot products.

By taking a look at Fig. 13-b, and -c, it can be seen that the shock and other features of the flow occur at the same time. Figure 13-b shows the pressure gradient magnitude in the flow field, and Fig. 13-c, shows the density gradient, and these two parameters are the most important elements in the DDT phenomena. Overall, Fig. 13 shows a strong shock wave propagating ahead of the flame front. After its interaction with the flame front, a Mach steam was generated and acted as the leading shock. A group of shock waves propagated down the channel before the flame arrival. These shocks diffract around the obstacles, inducing flow and enhancing shear layer turbulence behind the obstacle plates. As a result of the interaction of Mach stem with a transverse shock wave and the incident shock, a triple point has been generated in the flow field (which can be seen in Fig. 13-b). Moreover, due to the generation of the secondary transverse shock wave and interaction of this wave with the secondary Mach stem and the reflected shock wave, another triple point appeared in the flow field, which can be seen in Fig. 13-b and named as a secondary triple point.

It is known that Baroclinic vorticity generation due to non-parallel gradients in the pressure and density fields can enhance flame wrinkling on small scales and macroscopic flame

distortion on large scales. Thomas et al. (2001) experimentally demonstrated the great potential of shock-flame interaction in flame acceleration. Kholkhlov et al. (1999) likewise found that shock-flame interaction is important to accelerate flames to critical conditions for the onset of detonation. They believe large scale RM instability was the primary mechanism increasing the heat release rate during the interaction of a flame with a single shock through macroscopic flame surface area growth while small-scale instability decays quickly and hence can only contribute for a short time.

6. Conclusions

Numerical studies have been conducted to investigate DDT of a non-homogenous mixture of hydrogen-air in an obstructed channel with both 30% and 60% BR. The predicted flame position and flame tip speed are in reasonably good agreement with the measurements of Boeck et al. (2015). Qualitatively the predicted density fields are in line with the recorded density Schlieren. The first localized explosion occurred near the bottom wall where the shock and flame interacted, and the mixture was most lean and then the second localized explosion is took place at the top wall due to the reflection of shock and flame front which is in the region and later develops to form the leading detonation wave. The increase in the BR was found to increase the FA and slow down the possibility of transition to detonation in the present configuration.

The role of hydrodynamic instabilities and the effect of baroclinic torque and RM instability have also been studied. The forward jet and backward jets which are a mushroom form flow, represent the RM instability on the interface between the burned and unburned gas. The forward jets were found to impact on the shock front causing the appearance of a secondary triple point on the initial Mach stem on the flame front. The forward jet in the first shear layer was found to be consumed faster than those in the secondary shear layer. On the contrary, the backward jet consumed slower in the first shear layer than in the secondary shear layer. This is thought to be due to the existence of an unburned gas region between these two shear layers. The jets moving toward the burned pockets are moving slower than those going towards the unburned gas. The results support that RM instability is the primary source of turbulence generation in the present case.

Acknowledgement

This research is part of a research project dedicated to safer production and transportation of LNG termed as SafeLNG. This project is supported and funded by the European Commission, Marie Curie Actions.

References

Boeck, L.R., Katzy, P., Hasslberger, J., Kink, A., Sattelmayer, T., 2015. The "GraVent DDT Database". 25th International Colloquium on the Dynamics of Explosions and Reactive Systems (ICDERS), Leeds, UK.

Brouillette, M., 2002. the richtmyer-meshkov instability. Annu. Rev. Fluid Mech., 34, 445–468.

Ciccarelli, G., Boccio, J.L., 1998. Detonation wave propagation through a single orifice plate in a circular tube. Proc. Combust. Inst., 27 (2), 2233–2239.

Ciccarelli, G., Dorofeev, S., 2008. Flame acceleration and transition to detonation in ducts. Prog. Energy Combust. Sci., 34 (4), 499–550.

Cloutman, L.D., Wehner, M.F., 1992. Numerical simulation of Richtmyer–Meshkov instabilities. Phys. Fluid, 4, 1821–1830.

Ersen, K.K., 2004. Gas explosions in process pipes. PhD thesis, Telemark University College, Norway.

Ettner, F., Vollmer, K.G., Sattelmayer, T., 2014. Numerical Simulation of the Deflagration-to-Detonation Transition in Inhomogeneous Mixtures. J. Combustion, Article ID 686347.

Khokhlov, A.M., Oran, E.S., Thomas, G.O., 1999. Numerical simulation of deflagration-to-detonation transition: the role of shock–flame interactions in turbulent flames. Combust. Flame, 117, 323–339.

Khokhlov, A.M., Oran, E.S., Chtchelkanova, A.Y., Wheeler, J.C., 1999. Interaction of a shock with a sinusoidally perturbed flame. Combust. Flame 117, 99–116.

Li, X.L., Zhang, Q., 1997. A comparative numerical study of the Richtmyer–Meshkov instability with non linear analysis in two and three dimensions. Phys. Fluid 9, 3069–3077.

Mahmoudi, Y., Mazaheri, K., Parvar, S., 2013. Hydrodynamic instabilities and transverse waves in Propagation mechanism of gaseous detonations. Acta Astronautica 91, 263–282.

Mazaheri, K., Mahmoudi, Y., Radulescu, M.I., 2012. Diffusion and hydrodynamic instabilities in gaseous detonations. Combust. Flame 159, 2138–2154.

OpenFOAM Ltd., OpenFOAM, Available from: http://www.openfoam.com/

OpenFOAM Wiki, “Limiters,” 2010, Available from: http://openfoamwiki.net/index.php/OpenFOAM_guide/Limiters.

Regele, J. D., 2013. Purely Gasdynamic Multidimensional Indirect Detonation Initiation Using Localized Acoustic Timescale Power Deposition. Aerospace Sciences Meeting including the New Horizons Forum and Aerospace Exposition, 51st AIAA, 1172.

Sod, G. A., 1978. A Survey of Several Finite Difference Methods for Systems of Nonlinear Hyperbolic Conservation Laws. J. Comput. Phys. 27, 1–31.

Gamezo, V.N., Ogawa, T., Oran, E.S., 2007. Numerical simulations of flame propagation and DDT in obstructed channels filled with hydrogen–air mixture. Proceedings of the Combustion Institute 31, 2463–2471.

Kumar, P. P., Kim, K.S., Oh, S., Choi, J.Y., 2015. Numerical comparison of hydrogen-air reaction mechanisms for unsteady shock induced combustion applications. J. Mechanical Science and Technology 29 (3), 893-898.

Stamps, D. W., Benedick, W. B., Tieszen, S. R., 1991. Hydrogen-Air-Diluent Detonation Study for Nuclear Reactor Safety Analyses. Report no. SAND89-2398, Sandia National Laboratories, USA.

Thomas, G., Bambrey, R., Brown, C., 2001. Experimental observations of flame acceleration and transition to detonation following shock-flame interaction. Combustion Theory and Modelling 5 (4), 573–594.

Thomas, G.O., 2012. Some observations on the initiation and onset of detonation. Philosophical transactions series A, Mathematical, physical, and engineering sciences, 370 (1960), 715–39.

Ukai, S., Balakrishnan, K., Menon, S., 2011. Growth rate predictions of single- and multi-mode Richtmyer–Meshkov instability with reshock. Shock Waves 21 (6), 533-546.

Vetter, M. and Sturtevant, B., 1995. Experiments on the Richtmyer-Meshkov instability of an air/SF6 interface. Shock Waves 4, 247-252.

Wang, C. J., Wen, J. X., ShouXiang, L.U., Jin, G.U., 2012. Single-step chemistry model and transport coefficient model for hydrogen combustion. Science China Technological Sciences 55 (8), 2163-2168.

- Numerical studies have been conducted to investigate DDT of non-homogenous mixture.
- The first localized explosion occurred near the bottom wall where the mixture is lean.
- The increase in the BR was found to increase the flame acceleration.
- The role of hydrodynamic instabilities in DDT phenomena have also been studied.